

Pürüzlülük Kaynaklı İlave Gemi Direncin CFD ile Belirlenmesi

Anders Östman¹, Kourosh Koushan², Luca Savio³

anders.ostman@sintef.no¹, kourosh.koushan@sintef.no², luca.savio@sintef.no³

^{1,2,3} SINTEF Ocean, Trondheim/Norway

ÖZET

Pürüzlülükten kaynaklanan ek direnç CFD simülasyonları ile incelenmiştir. Tam ölçekli Reynolds sayısındaki KVLCC2 bir test durumu olarak kabul edilir. Türbülanslı sınır katmanını modellemek için bir duvar fonksiyonu formülasyonu kullanılır. Burada pürüzlülük fonksiyonu, tam ölçekli gemide olduğu gibi benzer pürüzlülükte boya ile kaplanmış çekme düz plakalarından elde edilen verilere dayanır. Çeşitli pürüzlülük yüksekliğine sahip kaplamalar için ilave direnç, 10 μm 'den 60 μm 'ye kadar değişen pürüzlülük yükseklikleri ile incelenmiştir. Ayrıca, sürtünme direncinin düşük maliyetli azaltılmasındaki potansiyel araştırılmıştır. Gövde sürtünmesinin yüksek olduğu belirli yerlere yüksek kalitede boya kaplama (düşük pürüzlülüğe sahip) uygulanabilirken, gövde sürtünmesinin daha az önemli olduğu diğer yerlerde daha ucuz kaplama ve uygulama prosedürleri (daha büyük yüzey pürüzlülüğü ile sonuçlanan) kullanılabilir.

Anahtar kelimeler: CFD, gemi direnci, yüzey pürüzlülüğü

Makale geçmişi: Geliş 10/12/2019 – Kabul 21/12/2019

Study on Additional Ship Resistance due to Roughness using CFD

Anders Östman¹, Kouros Koushan², Luca Savio³

anders.ostman@sintef.no¹, kouros.koushan@sintef.no², luca.savio@sintef.no³

^{1,2,3} SINTEF Ocean, Trondheim/Norway

ABSTRACT

The additional resistance due to roughness is studied by means of CFD simulations. The KVLCC2 hull at full-scale Reynolds number is considered as a test case. A wall function formulation is used to model the rough wall turbulent boundary layer, where the roughness function is based on data from towing flat plates coated with paint of similar roughness as for the full-scale vessel. The additional resistance for coatings with various roughness heights is studied, with roughness heights ranging from less than 10 μm to more than 60 μm . Also, the potential in low-cost reduction of frictional resistance is investigated. High-quality paint coating (with low roughness) can be applied at given locations where the skin friction is high, while using cheaper coating and application procedures (resulting in larger surface roughness) at other locations where skin friction is of less importance.

Keywords: CFD, ship resistance, surface roughness

Article history: Received 10/12/2019 – Accepted 21/12/2019

1. Introduction

Resistance due to fouling and poorly applied antifouling coating can have a significant contribution to the total resistance of a ship. This is especially true for ships operating at low Froude numbers, where skin friction resistance is the dominating component of the hydrodynamic resistance and could account for 60% or more of the total resistance. Reliable estimations of added resistance due to rough hull surfaces are important in order to be able to perform speed prediction of the vessel. Also, insight into the relative importance of roughness at different parts of the hull can be used to give guidance on where and how to apply antifouling coating on the ship.

Numerical simulations of rough surface friction drag are traditionally based on roughness functions that relies on finding an equivalent sand grain height that fits Nikuradse (1933) pipe flow experiments, examples can be found in Vargas and Shan (2016) and Demirel et al (2014).

In the present paper a different approach is applied, the roughness function is based directly on experimental resistance test of the specific surface coating. The roughness function is derived based on experimental flat plate towing tank tests. Plates with various surface roughness were towed at constant speeds, Savio et al (2015), and the results were post processed using methods proposed by Granville (1987). The roughness levels of the different plates were related to typical real applications processes used in the marine industry. Results from these tests were implemented in customized rough wall functions in the OpenFOAM flow solver, and presented in a validation study, Östman et al (2017). The validation showed very good agreement of computed flat plate resistance against experiments.

The method is in the present paper applied on a full-scale ship hull. The coatings and roughness models developed in the 2D validation study is used to model the rough surface ship hull. The computed total friction resistance of the various coatings is compared. Also, the effect of applying the highest quality coating at limited areas, selected based on the computed friction coefficient, is studied.

2. Formulation of the Roughness Wall Function

The implemented physical model that is used to model rough surfaces in the CFD simulations relies on measured flat plate resistance experimental results. Flat plates with various surface roughness were towed at constant speed while resistance was recorded, Savio et al (2015). The roughness on the plates was due to paint applied on the surface of the plates with various quality of application process. The aim was to mimic typical real application processes used in the marine industry. Three roughness levels (denoted A, B and C with increasing order of roughness) were considered. Roughness level A represents an optimal new build or full blast dry docking application of the paint. Roughness level B corresponds to dry dock situation with some underlying spot repair roughness and poor coating application of the paint. Finally, the plate with the most severe roughness was denoted level C, which could simulate an extreme case with severe underlying roughness accumulated from several dry dockings and very poor application of the paint. In addition, a set of smooth blank plates were used in order to have a reference to the theoretical smooth boundary layer friction drag.

The measured drag was post-processed following methods proposed by Granville (1987) and presented in terms of inner variables, Fig.1. The graph shows the shift ΔU^+ of the velocity profile in the logarithmic part of the boundary layer as a function of the non-dimensional roughness height, k^+ , where k^+ is defined by $k^+ = kU\tau/v$. The height, k [m] is a typical roughness height of the rough surface, $U\tau$ is the friction velocity and v is the fluid kinematic viscosity. The variable, k^+ , can be interpreted as a local Reynolds number for the surface roughness in the boundary layer. The value of typical roughness height, k , is found from a statistical analysis of the actual rough surface and defined as the rms (root mean square) of absolute heights of the surface, and denoted S_q in the following. The statistics of the surface is found from analyzing high-resolution laser scan of imprints of the surface. The measured rms roughness height of the plates is presented in Table 1. Visualisations of the surface from the laser scan is shown in Fig.2.

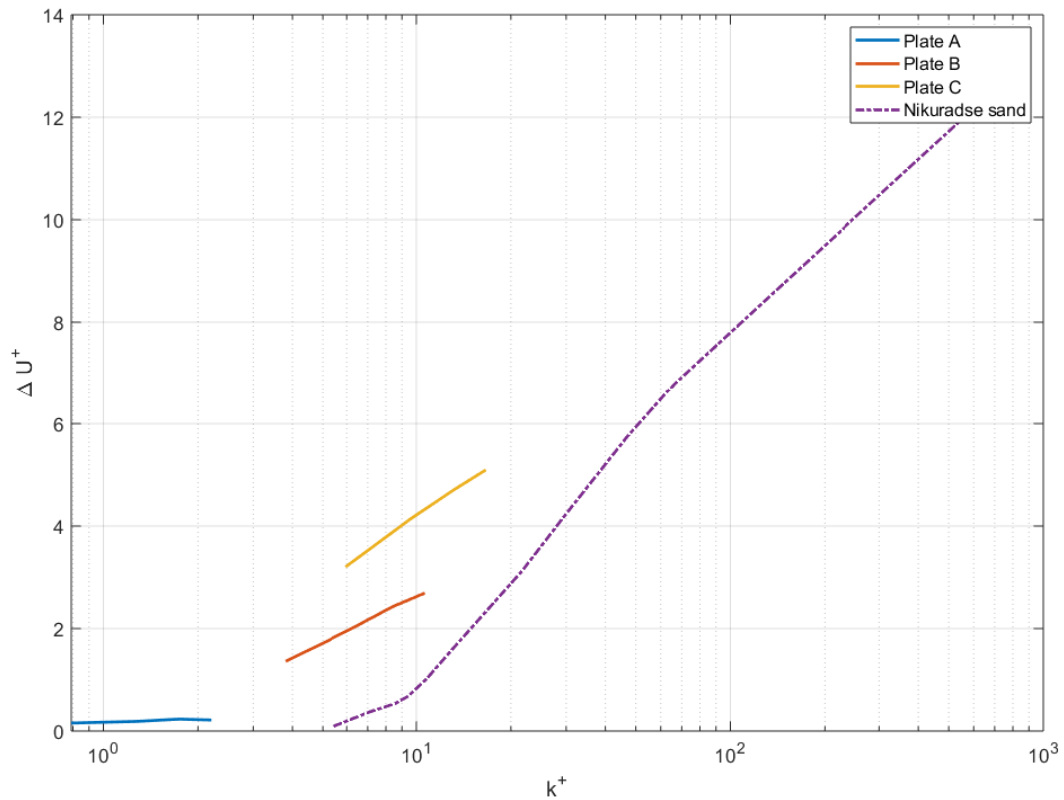


Fig. 1. Presentation of the experimental data in terms of inner variables

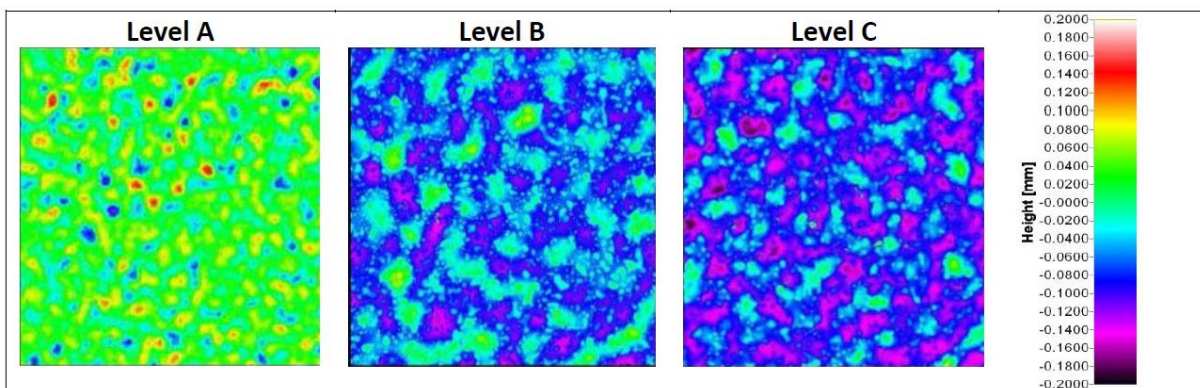


Fig. 2. Visualization of surface scans of the plates

Table 1. Measured root mean square of absolute heights of the surface roughness (Sq) of the plates

Plate	$Sq[\mu\text{m}]$
Plate A	8.51
Plate B	41.15
Plate C	64.44

The towing test results of the rough plates was used to derive the roughness function that is implemented in the CFD solver. The experimental results, Fig.1, show that each plate has a linear relation between velocity shift and $\log(k^+)$. Based on this observation, the idea of developing dedicated roughness functions for each surface coating was considered.

The velocity profile in the log law region is described by the equation, Cebeci and Bradshaw (1977):

$$U^+ = \frac{1}{\kappa} \ln(E y^+) \quad (1)$$

where $\kappa=0.41$ is the von Karman constant and E is a constant which equals 9.8 for smooth walls. For rough walls the velocity profile is switched downward in the logarithmic region. This can mathematically be expressed by substituting E with a modified variable E' defined as

$$E' = \frac{E}{f} \quad (2)$$

Where the roughness function, f , can be found directly based on experimental results of the velocity shift (ΔU^+). The procedure on how to estimate f directly from measurements are described in the following. Inserting the expression given in Eq. (2) into Eq. (1) gives:

$$U^+ = \frac{1}{\kappa} \ln\left(\frac{E}{f} y^+\right) = \frac{1}{\kappa} \ln(E y^+) - \frac{1}{\kappa} \ln(f y^+) \quad (3)$$

The last term in the equation is the velocity shift, ΔU^+

$$\Delta U^+ = \frac{1}{\kappa} \ln(f y^+) \quad (4)$$

ΔU^+ is defined to be positive when the velocity profile is shifted downwards. The roughness function f can now be found directly from Eq. (4):

$$f = e^{(\kappa \Delta U^+)} \quad (5)$$

As seen in the experimental results for the velocity shift that are presented in Fig.1 as a function of k^+ , it is evident that a logarithmic fit can be found for each plate. An expression of the velocity shift can be formulated as:

$$\Delta U^+ = a_0 + a_1 \log_{10}(k^+) \quad (6)$$

where a_0 and a_1 are constants of the curve fit. The best fit for different plates are shown in Fig.3.

3. CFD Solver

The flow solver used is the simpleFOAM mono fluid solver included in the OpenFOAM package. The solver solves the steady-state fluid flow using the SIMPLE algorithm, Ferziger and Peric (2002). The k -omega SST turbulence model is used to model turbulence. The flow over the rough surfaces is modeled by means of modifying the smooth wall function as described in the previous section.

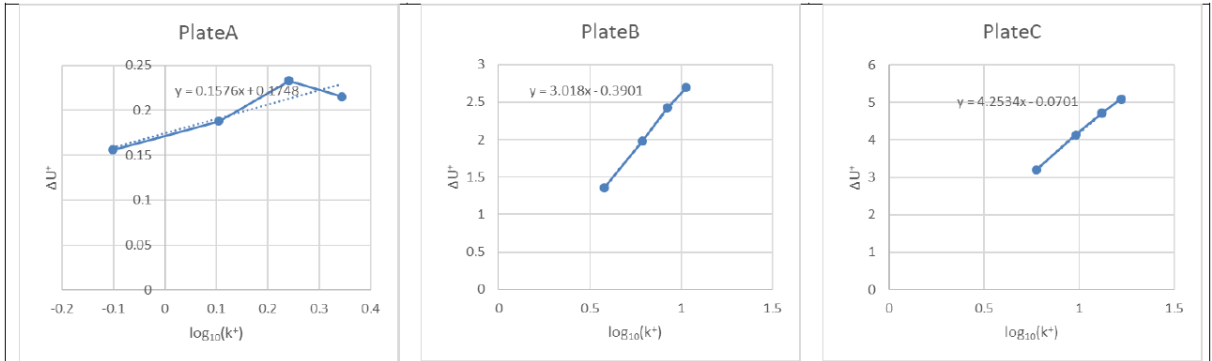


Fig. 3. Curve fit of measured velocity shift for the plates

4. Flat Plate Validation Study

The flat plate validation study, presented in Östman et al (2017), is in the following shortly summarized. The problem is simplified in the CFD analysis by neglecting wave generation and end-effects of the towed plates. This is done by solving the equations for a mono-fluid flow field in a 2D dimensional flow domain. Separate meshes were generated for each speed, the meshes were generated with a target for the near wall mesh spacing that results in $y^+ \approx 60$ for the cell center of the wall adjacent cells, Fig.4.

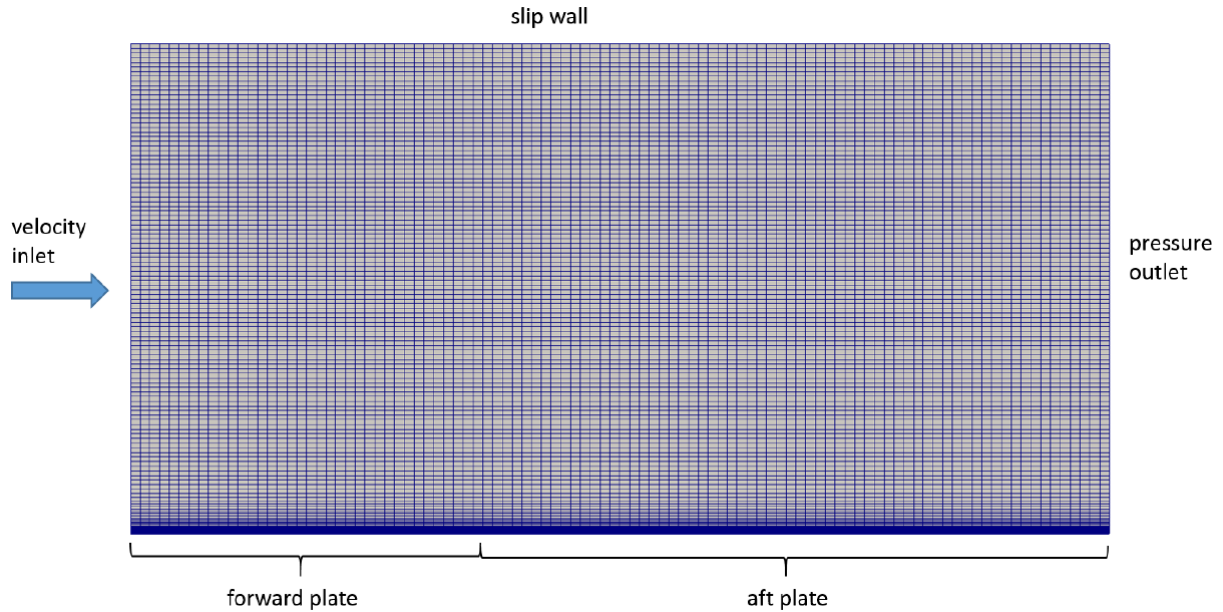


Fig.4. Mesh in the flow domain and boundary conditions

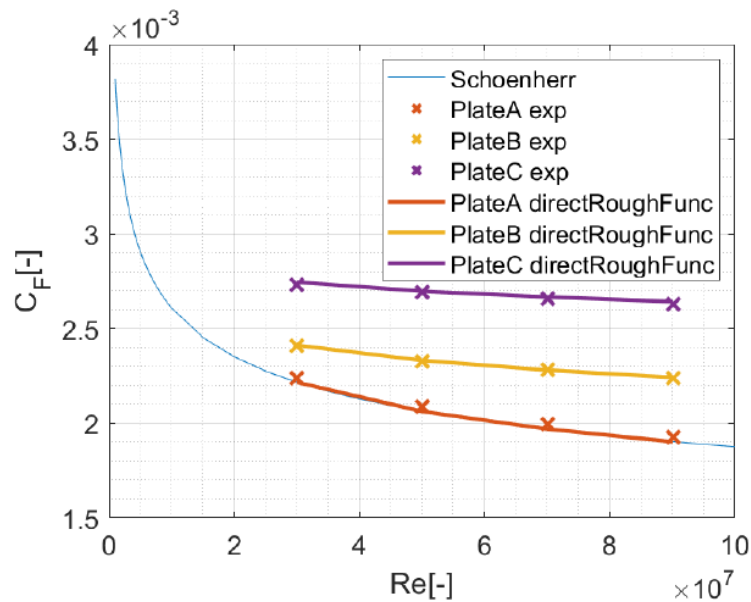


Fig. 5. Skin friction resistance coefficient. Comparison of CFD results using the direct roughness function formulation Eq.(5) against experimental results.

The simulations were performed for the same speeds as tested in the towing tank, $U=3, 5, 7$ and 9m/s . The computed results are compared against experiments in Fig.5. The comparison is very good for all plates. The implemented roughness function is thus able to accurately model the behavior of the rough surfaces.

5. Full Scale Ship Hull Simulations

Simulation of the full scale KVLCC2 hull is performed at 15 kn. The length between perpendiculars of the vessel is 320 m, resulting in a Reynolds number of 2.08×10^9 and Froude number 0.137. The same rough hull coatings as in the flat plates experiments is assumed. At this low Froude number, wave resistance is of less importance, while skin friction resistance being the dominant resistance component. The purpose of the present study is to quantify the increase in resistance due to hull surface roughness. It was therefore decided to simplify the simulation setup by replacing the free surface with a fixed slip surface. The motivation for this simplification is: (i) Changes in wave resistance due to hull surface roughness is assumed to be very small. The wave pattern, and hence, the wave resistance is not expected to be influenced by the hull surface roughness. (ii) We are only interested in the difference in resistance due to hull roughness, thus, the actual level of resistance is of less importance as long as the difference in resistance is captured by the simulation setup. (iii) The wave resistance is anyhow a small component of the total resistance due to the small Froude number.

The rough surface was modelled using the direct roughness function with the same parameters as for the flat plate simulations. The 3D volume mesh was generated using the HEXPRESSTM grid generator. Illustrations of the flow domain and mesh on the hull surface in the symmetry plane are shown in Fig.6 and Fig.7. The mesh is refined in the boundary layer in order to accurately capture the boundary layer profile. The aim is to have a y^+ value in the range 40-100 at the cell centre in vicinity to the hull surface. Based on boundary layer theory the size of the first cell normal to the hull surface is chosen as 0.6 mm. The total number of grid cells was approximately 6.2M.

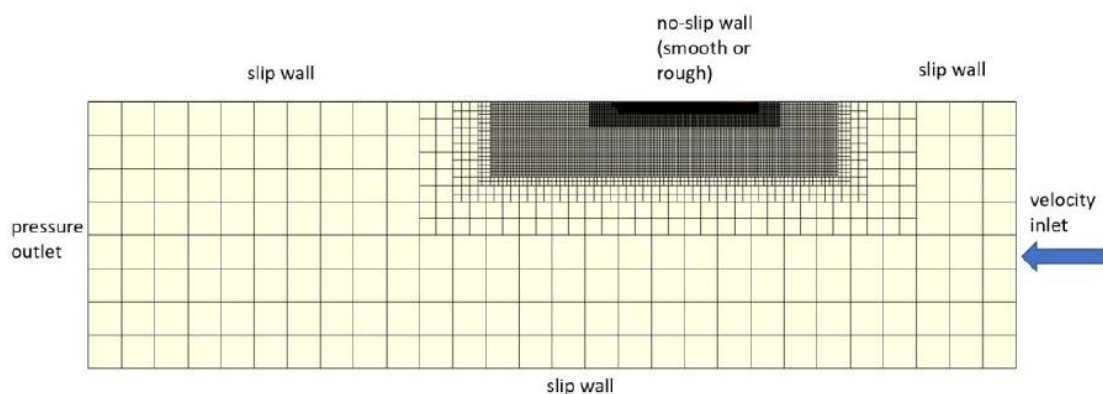


Fig. 6. Illustration of mesh on the hull surface and in the symmetry plane

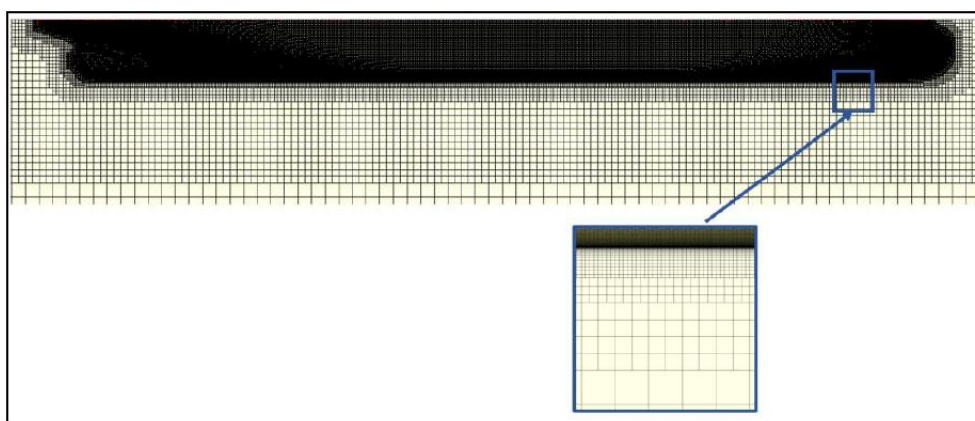


Fig. 7. Mesh on the hull surface and in the symmetry plane in vicinity to the hull

The computed wall shear stress on the hull for the different surface coatings is presented in Fig.8. For simplicity, the surfaces are denoted to have different coatings, this is strictly not correct, all surfaces are treated with the same coating, but using different quality of the application process, resulting in different surface roughness. However, the term "coating" is in the following used to simplify the presentation.

As expected, the wall shear increases with increasing surface roughness. Moreover, the increase in shear stress is seen on the entire hull surface. As was also observed in the flat plate simulations, the smoothest coating is very smooth, which results in a shear stress that is very similar to the stress on the hydraulic smooth reference surface. The largest values of wall shear stress are seen in areas with accelerations in the flow, such as around the shoulder and at the bilge in the bow area. The computed friction resistance coefficients are compared in Table 2. The increase in resistance for coating A, compared to the smooth surface, is only 0.9%. Coating B results in about 11% increase, while the increase in resistance for coating C is 24% compared to the smooth surface.

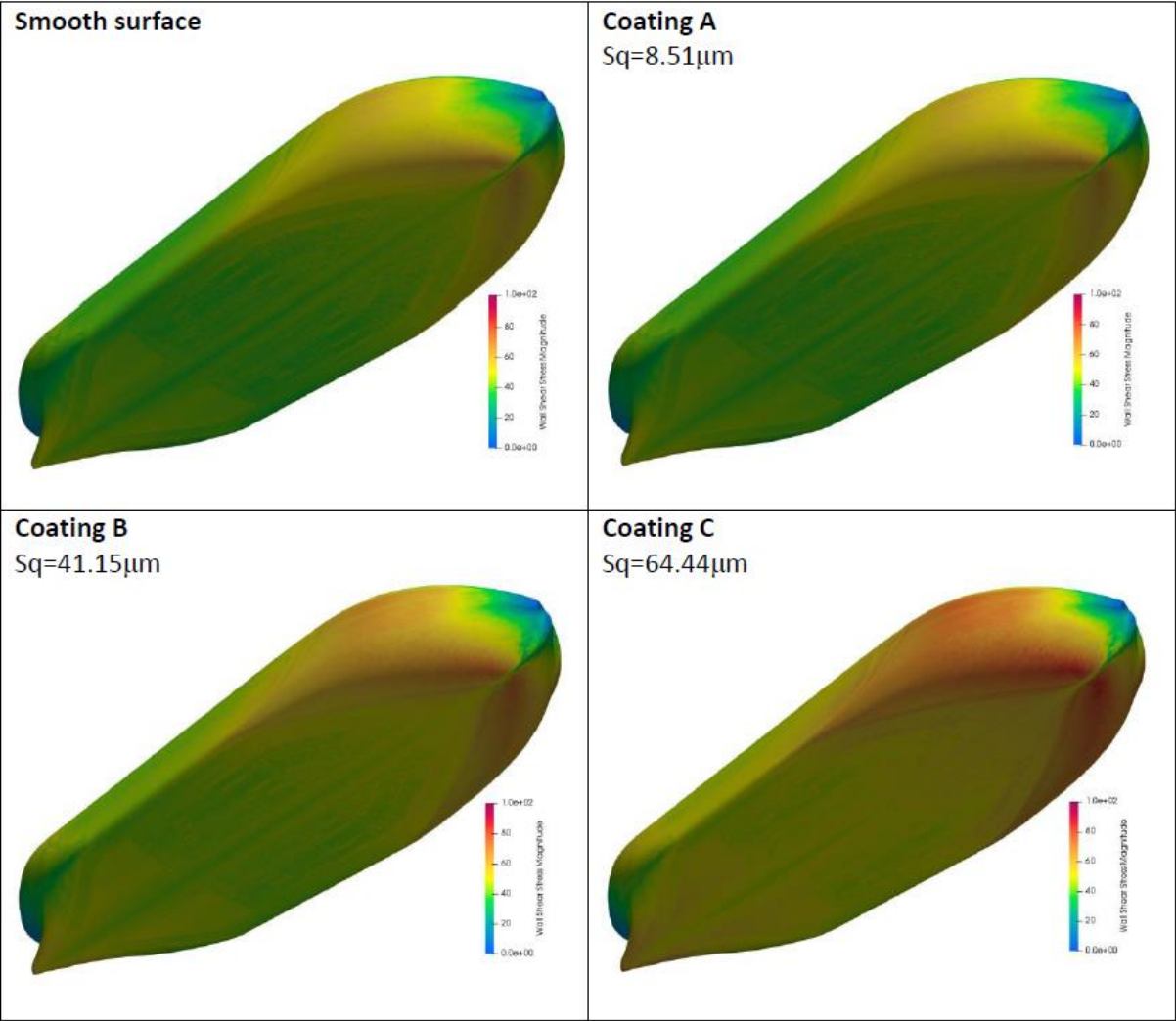


Fig. 8. Computed wall shear stress at the hull surface for the different coatings

In an attempt to investigate the relative importance of surface coating quality at different parts of the hull, the hull surface was split based on shear stress threshold values. Using coating C as a basis, areas with shear stress exceeding 60, 65 and 70 Pa were identified. The hull surface was thereafter split in

two parts based on these threshold values. The splits are shown in Fig.9. The red part illustrates areas with high wall shear stress. The size of the area of the high shear part of the hull depends on the threshold value. The area of the part of the hull where $\tau_w > 70$ Pa is 134 m², this corresponds to approximately 0.5% of the total wetted hull surface area. Threshold $\tau_w > 65$ Pa results in an area of 798 m² (3%), while $\tau_w > 60$ Pa results in an area of 2433 m² (9%). Simulations were thereafter performed using the high quality coating A at the part of the hull where the shear stress exceeds the threshold value, while the remaining part of the hull has the rough coating C. The computed wall shear stress on the hull surface is also shown in the figure. The shear stress is significantly reduced at areas where the smooth coating is applied.

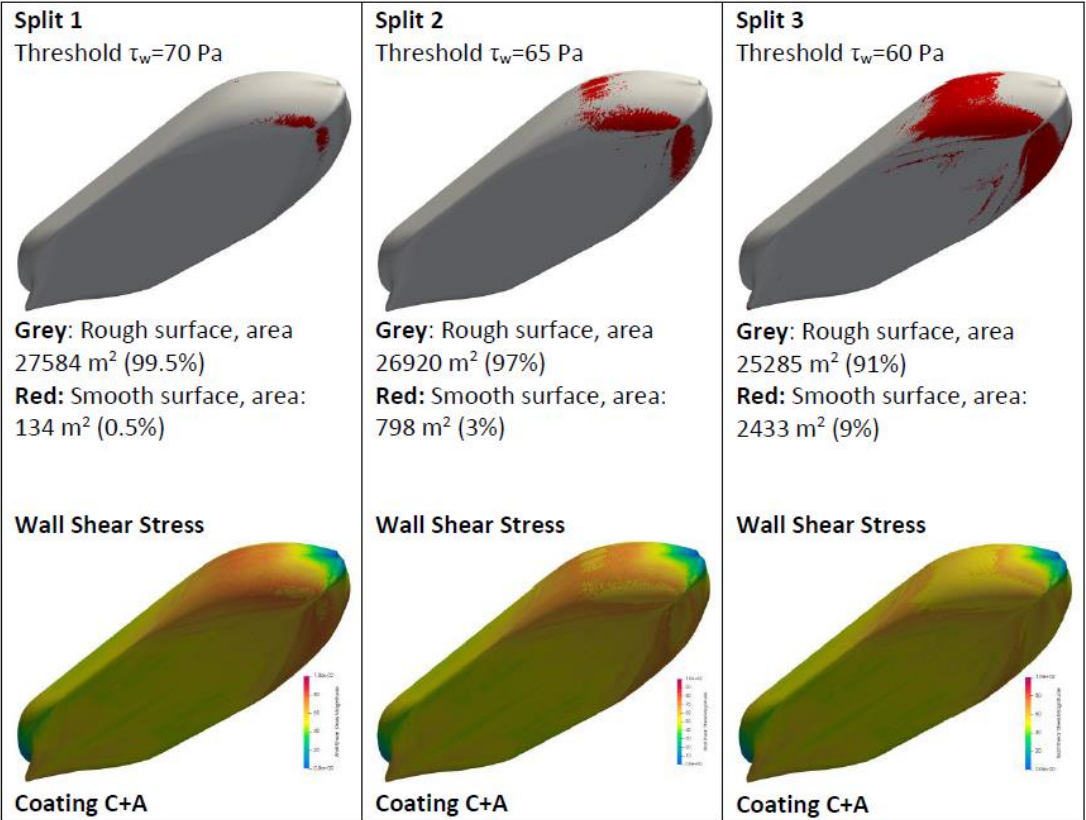


Fig. 9. Above: The hull surface splitted based on a wall shear stress threshold. Below: Computed wall shear stress at the hull surface. Simulations using different coatings. Surface coating C is applied on the grey part of the hull, coating A is applied on the red part.

Table 2. Computed friction resistance coefficient of hull with different coatings. The increase relative to the smooth hull is also presented.

Surface description	$C_f * 1000$ [-]	% Increase
Smooth	1.3096	0.0 %
Coating A	1.3216	0.9 %
Coating B	1.4502	10.7 %
Coating C	1.6240	24.0 %
Split 1, Mixed Coating C+A	1.6219	23.8 %
Split 2, Mixed Coating C+A	1.6151	23.3 %
Split 3, Mixed Coating C+A	1.5905	21.4 %

The computed friction resistance coefficients are presented in Table 2. The resistance is reduced for the hull with mixed coatings compared to the hull with coating C. However, the reduction is not very large. For Split 1, where only 0.5% of the hull is treated with coating A while the rest of the hull consist of coating C, the increased resistance compared to the smooth reference is 23.8%, instead of 24% for the hull with coating C on the entire wetted surface. This corresponds to approximately 1% "reduction of increase" (0.2% of 24%). That is, by treating 0.5% of hull with a high-quality coating, the increase in resistance is reduced by 1%. By increasing the area of the part which is coated with coating A the resistance is further reduced. For Split 3, where 9% of the hull is treated with coating A, the increase in resistance is reduced to 21.4 % compared to the smooth surface hull simulations. The computed resistance of the various surface coatings is also compared in Fig.10.

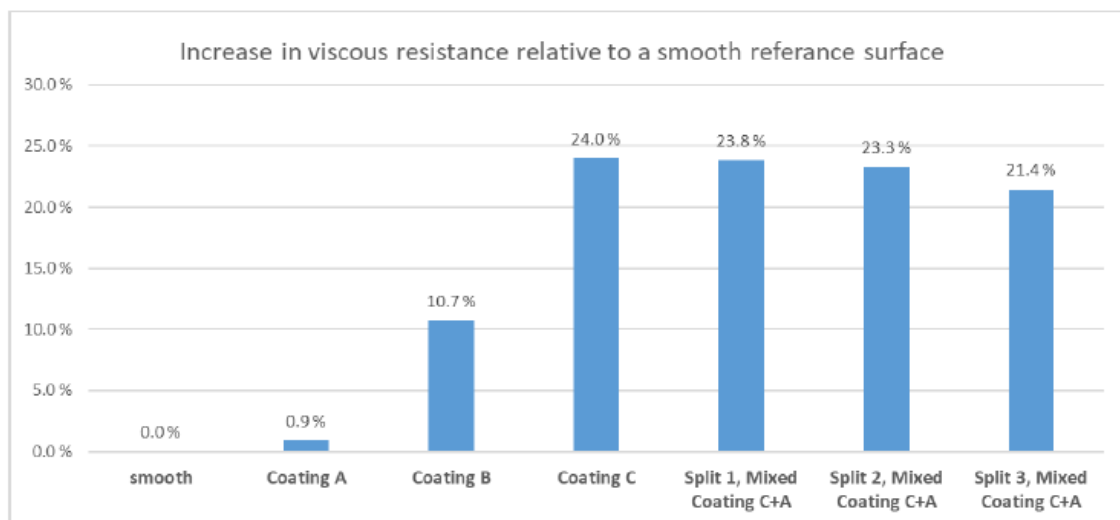


Fig. 10. Computed increase in viscous resistance for the different coatings

6. Conclusions

The additional viscous resistance due to surface roughness on a full-scale ship hull has been studied using CFD simulations. Three different rough coatings were modeled, the rough surfaces correspond to realistic hull surface conditions found in the marine industry. Parameters in the numerical implementation of the roughness function, which is used in the turbulent wall function, relies on towing tank experiments conducted on coated sample plates.

The simulations showed, for the roughest coating, an increase in viscous resistance of 24%, compared to a smooth hull surface. The potential of low-cost reduction of frictional resistance was also investigated. When a low roughness coating was applied at locations where the shear stress is high, while the rest of the hull had a high roughness coating, the resistance was reduced compared to having the same rough coating on the entire hull. However, the reduction of viscous resistance was not very large. When 9% of the hull has a low roughness coating, while the rest of the hull is coated with the roughest coating, the increase in viscous resistance was computed 21.4%, instead of 24%, which is the increase in resistance when the entire hull is coated with the roughest coating.

Acknowledgements

Part of this work was supported by the EU FP7 Project "Low-toxic cost-efficient environment-friendly antifouling materials" (BYEFOULING) under Grant Agreement no. 612717.

7. References

Cebeci, T.; Bradshaw, P. (1977), *Momentum Transfer in Boundary Layers*, McGraw-Hill

Demirel, Y.K.; Khorasanchi, M.; Turan, O.; Incecik, A. (2014), A CFD model for the frictional resistance prediction for antifouling coatings, *Ocean Engineering* 89, pp.21-31

Ferziger, J.H.; Peric, M. (2002), *Computational Methods for Fluid Dynamics*, Springer

Granville, P.S. (1987), Three Indirect Methods for the Drag Characterization of Arbitrarily Rough Surfaces on Flat Plates, *J. Ship Research* 31, pp.70-77

Grigson, C.W.B. (1992), Drag losses of new ships caused by hull finish, *J. Ship Res.* 36, pp.182– 196

Nikuradse, J. (1933), *Laws of flow in rough pipes*, NACA Technical Memorandum 1292

Östman, A.; Koushan, K.; Savio, L. (2017), Numerical and Experimental Investigation of Roughness Due to Different Type of Coating, 2nd HullPIC, Ulrichshusen

Savio, L.; Berge, B.O.; Koushan, K.; Axelsson, M. (2015), Measurements of added resistance due to increased roughness on flat plates, 4th Int. Conf. Advanced Model Measurement Technology for the Maritime Industry, Istanbul

Vargas, A.; Shan, H. (2016), A numerical approach for modeling roughness for marine applications, FEDSM2016-7791, ASME 2016 Fluids Engineering Division Summer Meeting, Washington